Measurement accuracy of the diameter of a carbon nanotube from TEM images

Chen Qin[1] and L.-M. Peng[1,2,*]
[1]*Department of Electronics, Peking University, Beijing 100871, China*
[2]*Beijing Laboratory of Electron Microscopy, Institute of Physics and Center for Condensed Matter Physics, Chinese Academy of Sciences, P.O. Box 2724, Beijing 100080, China*
(Received 2 August 2001; revised manuscript received 8 November 2001; published 15 April 2002)

The image contrast of a single-walled carbon nanotube (SWCNT) is investigated via high resolution transmission electron microscopy (HRTEM) experiments and image simulations. It is found that the common practice of determining the tube diameter by measuring the two dark lines in the HRTEM image of a SWCNT is not very accurate, and this is especially so for tubes with diameters smaller than 1 nm. Depending on the imaging conditions, both amplitude contrast and phase contrast may be generated by a carbon nanotube in a HRTEM image. In images taken at the Scherzer defocus, a SWCNT usually appear as two dark lines corresponding to the two walls of the nanotube but in general the distance between the two dark lines is smaller than the real diameter of the SWCNT. The discrepancy between these two values varies with the size of the tube and the alignment of the tube relative to the electron beam, and can be as large as 30% for sub-nanometer carbon nanotubes. For tubes larger than 1.0 nm, the discrepancy is typically less than 10%. The phase contrast of a SWCNT changes with defocus condition. The reverse contrast appears at a small underfocus, while the two dark lines associated with the two walls of the SWCNT become broader for a large underfocus. For accurate nanotube diameter determination, we recommend that measurements based on HRTEM images should be combined with image simulations and structural relaxation of the atomic models of the carbon nanotubes.

DOI: 10.1103/PhysRevB.65.155431 PACS number(s): 81.07.De, 61.14.Dc, 68.37.Lp

I. INTRODUCTION

Since the first discovery in 1991 by S. Iijima,[1] carbon nanotubes have been extensively studied due to its fascinating structure and properties. The size and helicity of the nanotubes are two important parameters that affect nanotube's properties. Based on earlier tight-binding band structure calculations, it was concluded that a nanotube can behave similar to a metal or a semiconductor depending on its diameter and helicity.[2] However, experimentally it is not easy to determine these parameters directly. Raman scattering is a powerful tool in mapping the distribution of nanotube diameters, but only works for bulk samples.[3–5] Scanning tunnelling microscopy (STM) and atomic force microscopy (AFM) are good methods to show the surface structure of nanotubes,[6] but they cannot distinguish a single-walled carbon nanotube (SWCNT) from a multiwalled carbon nanotube (MWCNT). The most widely used tool for the study of carbon nanotubes is a transmission electron microscope (TEM). While the type and helicity of a nanotube can be determined using electron diffraction,[7,8] the sign of the chiral angles can be determined by dark-field electron microscopy.[9] High-resolution TEM (HRTEM) is the method which may not only be used to measure the size but also to ''see'' atom structure directly.[1,7,10] It is widely accepted that carbon nanotube (CNT) diameter can be determined by directly measuring the distance between two dark lines associated with a CNT in a HRTEM image. It is well known, however, that there exist many factors, such as the defocus value and the size of the objective aperture used, that can dramatically change the appearance of the HRTEM images. In this work we aim to study systematically how the imaging conditions affect the appearance of the images of CNT's and to answer the question as to how accurate can we measure the diameter of the CNT from HRTEM images.

II. EXPERIMENTAL

All HRTEM experimental images presented in this paper were obtained using a Philips field-emission gun (FEG) TEM equipped with a Gatan Image Filter (GIF) system for energy filtering and digital image recording (CM200/FEG). To avoid unnecessary coherent effects resulting from the use of the FEG, a convergent incident electron beam is employed. The carbon nanotubes used were prepared using the arc-discharge method and the specimens were kindly provided by Professor Z.N. Gu.[11] Atomic models of SWCNT's are first constructed geometrically, and the structures are relaxed or optimized using the MSI software CERIUS.[2] All image simulations were performed using the same software.

III. RESULTS

The image contrast of a CNT may be dominated by either amplitude contrast or by phase contrast depending on the imaging conditions. Amplitude contrast appears when a small objective aperture is used. Regions with higher mass density or stronger potential will scatter more electrons toward larger angular region and therefore be imaged as darker regions.[12] Phase contrast, on the other hand, arises from the differences in the phases of the electron waves scattered through a thin specimen. The phase contrast is not only very sensitive to many specimen factors, such as the thickness, orientation, and scattering power of the specimen, but also sensitive to the spherical aberration of the objective lens and the variations in the value of defocus.[13] For a general specimen with a moderate thickness there exists no direct relationship between the structure and the phase contrast image. One outstanding exception to the rule being structure images or HRTEM images taken under special imaging conditions. Under these special imaging conditions the structure images reveal directly the atomic structure of the sample being im-

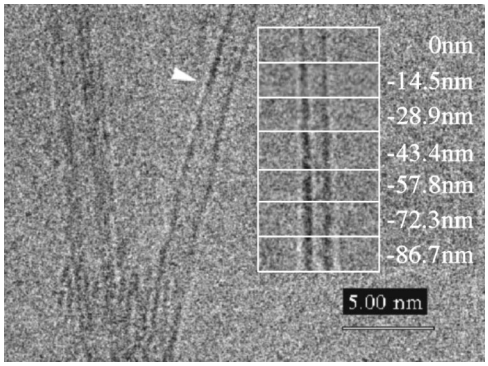

FIG. 1. Bright field image taken using a 0.23 $Å^{-1}$ objective aperture showing one single-wall carbon nanotube (right) and one double-wall carbon nanotube. The inserted smaller images are bright field images of the pointed area taken at the indicated defocus.

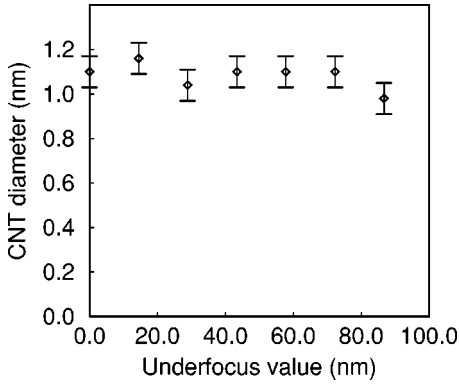

FIG. 2. The diameters of the same SWCNT measured from the bright field images taken at different underfocus values, i.e., with defocus values $\Delta f<0$.

aged and the conditions for obtaining structure images have been well documented.[14,15]

A. The amplitude contrasts

In imaging a SWCNT, the SWCNT is usually placed under the electron beam so that the tube axis is perpendicular to the incident electron beam. While around the central part of the SWCNT the incident electrons always ''see'' two sheets of graphitic carbon atoms in passing through the tube, the situation is less well defined toward the edges of the tube. It is a rule, however, that toward the edges of the tube and along the incident electron beam direction the mass density is higher than that in the central part of the tube. Amplitude contrast is then expected to result from the use of a small objective aperture and the mass density variation found in the SWCNT. On the other hand, since the orientation of the center part of a SWCNT and that at the edge of the tube are different relative to the incident beam, one expects that this orientation difference results in different diffraction conditions at different regions of the tube and different contrast in the final image. These two contrast mechanisms responsible together for the observed amplitude contrast of a SWCNT and the contrast may be enhanced by using a small objective aperture.

Shown in Fig. 1 is a bright-field (BF) image showing some carbon nanotubes (CNT's), in which the CNT marked by the white arrow is a SWCNT. In imaging these CNT's, a small objective aperture with a radius of 0.23 $Å^{-1}$ centered around the transmitted beam was used. Since this objective aperture is small, it blocks all the Bragg diffracted beams from CNT's and prevents them from contributing to the image contrast. The contrast of the image results therefore mainly from amplitude contrast. Inserted in the figure are BF images of the SWCNT to the right of Fig. 1 taken at different defocus values which are also given in the figure in addition to the inserted images. The diameter of the SWCNT being imaged is about 1.1 nm. Figure 1 clearly shows that the SWCNT appears as two dark lines in all inserted BF images taken at different defocus values. The dark lines become broader as the defocus value decreases. The distance between the center of the two dark lines is measured from these images, and the result is shown in Fig. 2.

In Fig. 2 the horizontal axis denotes the nominated underfocus value, read directly from the electron microscope. The vertical axis represents the measured distances between the two dark lines appearing in the BF images taken at different defocus conditions. This figure shows that different measurements from images taken under different imaging conditions give the same diameter of the SWNT within the experimental error (due mainly to the finite pixel size). It should be noted, however, that in addition to the experimental error, the resolution of these BF images is limited by the size of the objective aperture used. For a 0.23 $Å^{-1}$ objective aperture, the image resolution is not expected to be better than 4 Å. Therefore, although the measured result based on the amplitude contrast is not very sensitive to the experimental condition, it is not very useful for accurate measurement of the diameter of the CNTs due to the very limited resolution of the BF images.

B. The phase contrast and Scherzer images

Unlike the amplitude contrast, the phase contrast by its very nature is sensitive to the relative phases of diffracted electron beams and therefore the defocus values. In forming a phase contrast image a large objective aperture is usually used which allow diffracted electron beams to pass through the electron microscope column and contribute to the final image. The phase contrast image may therefore in principle provide higher resolution information on the CNT's being imaged and usually the phase contrast image of the CNT is called the HRTEM image.

Almost all electron microscopy images of CNT's found in the literature are phase contrast images, and it is a common practice to assume that the tube diameter may be measured from these phase contrast images when the electron beam is incident along a direction which is perpendicular to the tube. Although this ideal imaging condition may not always be satisfied when recording experimental images, since many CNT's coexist in the sample and most of them are inclined to the incident electron beam, we will first consider images taken at the ideal experimental conditions and in particular

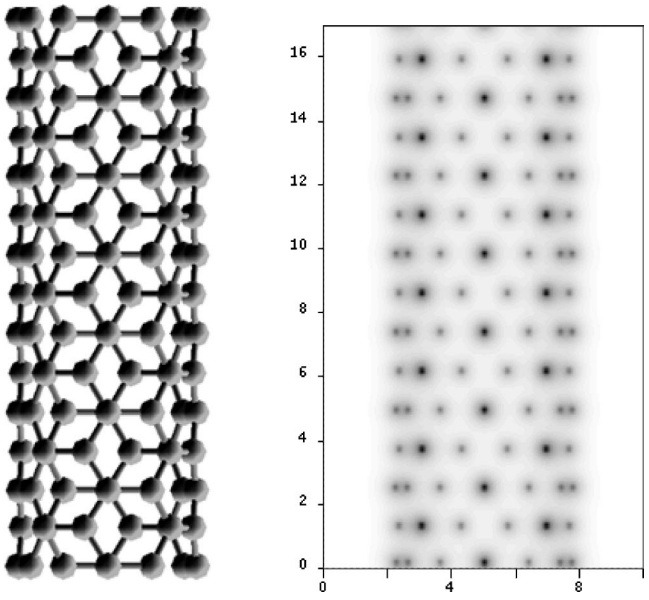

FIG. 3. Atomic model and corresponding projected potential along the incident electron beam direction for a (4,4) SWCNT.

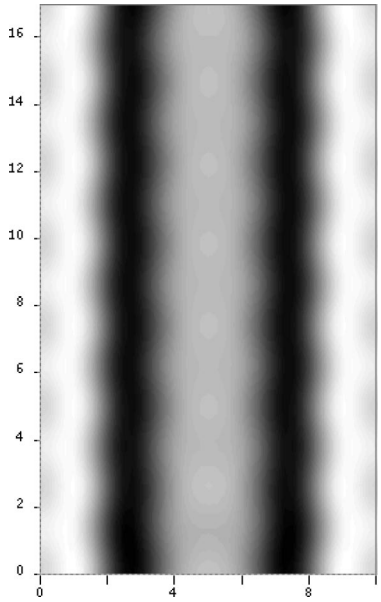

FIG. 4. Simulated high resolution image of a (4,4) SWCNT. The simulation was done for the 200 keV primary beam energy and the Scherzer defocus, using the CERIUS (Ref. 2) program. The two walls of the SWCNT appear as two dark lines.

images taken at the Scherzer defocus (in this paper we follow the notation employed in the CERIUS program[2] and define the Scherzer defocus as $\Delta f_s = -\sqrt{C_s \lambda}$. For 200 keV and a $C_s = 1.2$ mm this definition gives $\Delta f_s = -548.6$ Å) and defer discussions on the effect of using different defocus to the next subsection.

According to the weak phase object approximation (WPOA) theory,[14] a thin specimen may be represented by its projected potential along the electron beam direction. A SWCNT regardless of its diameter has only two atomic layers in the beam direction except at the edges of the tube, and to a good approximation a SWCNT may be regarded as a weak phase object. Using an ideal TEM, such as the recently developed spherical abberation free electron microscope,[16] a high resolution structural image may be obtained of the SWCNT and may be related directly to the projected potential of the SWCNT. Ignoring image deterioration due to the energy spread of the incident electron beam and finite vibration of the electron microscope, the projected potential may then be regarded as the ultimate image of a CNT. Projected potentials have been calculated for several types of SWCNT's using the CERIUS program,[2] and shown in Fig. 3 are the atomic model and corresponding projected potential for a (4,4) SWCNT. For this particular SWCNT and along this particular direction, the atomic positions of the top and bottom graphitic sheets overlap enhancing the projected potential at the overlapping atomic positions. All atom strings along the incident electron beam direction have be clearly resolved in Fig. 3, and the diameter of the CNT may be measured directly from the images of the outmost atom strings.

No electron microscope is perfect. All electron microscopes are subject to imperfections resulting from various kinds of factors, including spherical aberration, chromatic aberration, distortion, vibrations, and electron energy spread. In the most favorite cases, these imperfections introduce only a blurring to the image, and to a good approximation the blurring may be regarded as a convolution of the ideal image such as the one shown in Fig. 3 (the projected potential) with a spherically symmetrical point spread function. The point-spread function of the electron microscope transforms a point in specimen into a disk in the image plane. Figure 4 shows a simulated high resolution image of a (4,4) CNT for a 200 keV microscope using CERIUS with $C_s = 0.5$ mm,[2] a Scherzer defocus value of -354 Å and an aperture size 0.8 $Å^{-1}$. Distinct peaks due to different atom strings in the projected potential start to overlap in the simulated image and two prominent dark lines appear around the edges and along the axis of the CNT.

To find the relationship between the image and the projected potential, the projected potential distribution is averaged along the tube axis and compared with that of the simulated images. Figures 5 and 6 show line profiles of the averaged projected potential and the image intensity for two typical SWCNT's. Figure 5 shows results for a (4,0) SWCNT. It is seen that there exists only one minimum in the projected potential on each side of the (4,0) SWCNT, and that the centers of the dark lines in the image coincide with the minimum positions of the projected potential. In this particular case, the measured distance between the two dark lines appearing in the simulated image equals the distance between the centers of the projected potential minima. This is, however, not a generally correct fact. Shown in Fig. 6 are relevant line profiles of the projected potential and simulated image for a (4,4) SWCNT. For this tube the projected potential profile across the tube shows more than one minimum on each side of the tube. Nevertheless the centers of the image line profile fall roughly with the projected potential. Several simulations and comparisons have been made, and the results are listed in Table I.

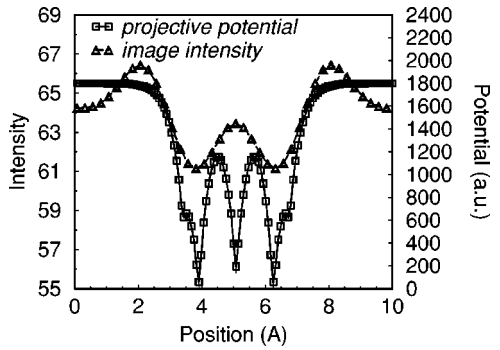

FIG. 5. Averaged projected potential and corresponding image intensity profile across a (4,0) SWCNT. The average is made along the tube axis and the darkest points of the averaged image coincide with the minima of the projected potential.

In Table I, "d_m" denotes the true diameter of the SWCNT model used in the image simulation; "d_{image}" denotes the measured diameter based on the two dark lines appearing in the simulated image; "$d_{p_{\text{in}}}$" denotes the measured distance between the inner minimums in the line profile of the projected potential; and "$d_{p_{\text{out}}}$" denotes that of the outer minimums of the projected potential. The distance between the outer minimums of the projected potential, i.e., measured $d_{p_{\text{out}}}$, is plotted in Fig. 7 as a function of the tube diameter together with relative errors.

A general statement that one can make regarding the measured diameters of the SWCNT's is that the measured diameter is in general smaller than the true diameter of the tube, and the discrepancy is an intrinsic one regardless of the accuracy of the measurement or the imperfection of the instruments, i.e., the error will exist even if one can make a perfect measurement. This intrinsic error results simply from the fact that the minimum in the total projected potential of a tube does not coincide with the position of the outmost atom of the tube. It is the latter which defines the diameter of the tube instead of the former and there exists no simple relationship between the two. While this intrinsic error is typically less than 10% for tubes with diameter larger than 1.0 nm, it can be as large as 30% for tubes with smaller diameters.[17–20]

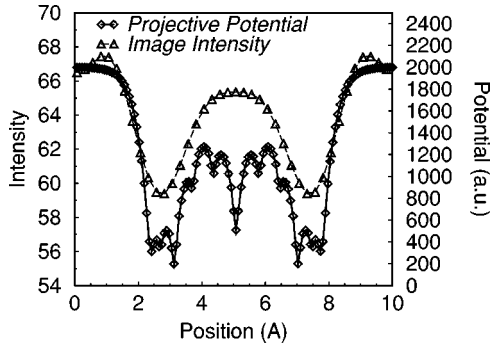

FIG. 6. Averaged projected potential and corresponding image intensity profile across a (4,4) SWCNT. The average is made along the tube axis, and the darkest points of the projected potential are not coincident with the minimum positions of the projected potential.

TABLE I. Diameters of several (n,m) SWCNT's.

n	m	d_m	d_{image}	$d_{p_{\text{in}}}$	$d_{p_{\text{out}}}$
4	0	0.334	0.25	0.224	0.224
5	0	0.404	0.30	0.125	0.328
3	3	0.421	0.30	0.211	0.399
6	0	0.478	0.375	0.412	0.412
4	4	0.550	0.475	0.390	0.531
8	8	1.084	1.00	1.026	1.026
11	11	1.487	1.41	1.453	1.453

While curves such as those shown in Fig. 7 may be used to correct for the intrinsic error, further complication arises from the relative direction of the incident electron beam and crystallographic orientation of the tube.

In all previously presented results, we have fixed the incident electron beam direction relative to the tube. As the tube size gets smaller, however, the projected potential will be different for different incident directions. Figure 8 shows the atomic model of a (4,4) SWCNT looking down along the tube axis. Obviously, the projected atomic structure or potential of the tube along different incident beam directions (A, B, or C directions) will be different. The exact positions of the dark lines appearing in the image of the tube will change accordingly. For the (4,4) tube shown in Fig. 8 the distance between the two dark lines is about 7% smaller for an incidence along the direction C, which gives the smallest distance, than that for the direction A, which gives the largest distance.

So far, we have only considered the case when the tube axis is perpendicular to the incident electron beam. Two new effects may result when the tube is tilted away from this ideal direction. First, the sample height will be different for different parts of the nanotube along the tube axis. This effect can be taken into account using an effective defocus value. Typically the uncertainty in the defocus value resulting from this effect is less than 10 nm, and we will show in the next subsection that a 10 nm deviation from the Scherzer defocus value does not introduce an obvious difference in the

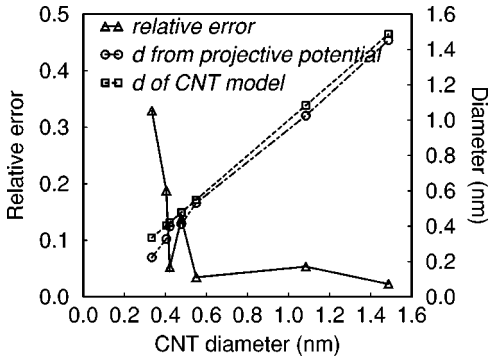

FIG. 7. The true diameters and the measured distances between the minimum positions in the averaged projected potential for several SWCNT's. Relative error is typically less than 10% for tubes larger than 1.0 nm but can be as high as 30% for tubes with smaller diameters.

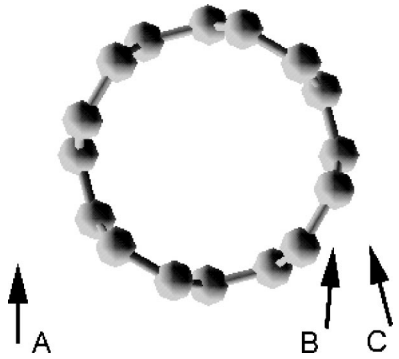

FIG. 8. Atomic model for a (4,4) SWCNT looking down along the tube axis. Projecting the tube along *A*, *B*, and *C* directions resulting in different projected potential distributions.

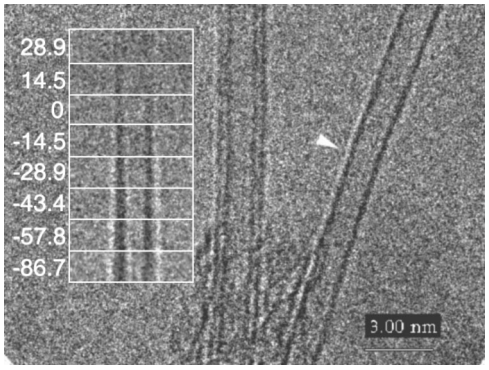

FIG. 9. High resolution experimental image of CNT's. The inserted images are experimental images from the arrow marked area taken at different defocus conditions. The indicated defocus values are in nm.

image contrast and therefore substantial error in measuring the diameter of a SWCNT. The second effect, resulting from the changes of the relative orientations between the incident electron beam and the atomic planes of the tube when the tube is tilted away from the ideal horizontal orientation (i.e., the direction perpendicular to the incident beam), is, however, not negligible. Detailed simulations shown that this effect can introduce additional error of more than 12% for a typical SWCNT and results on a (4,4) SWCNT are listed in Table II. In this table, ''tilting angle'' denotes the angle between the tube axis and the direction perpendicular to the incident electron beam; ''*d* measured'' denotes the measured diameter from the simulated HRTEM images; ''relative error'' denotes the error comparing with the true diameter ''d_{true}'' of the SWCNT model which is 0.55 nm for the (4,4) SWCNT. From Table II we see that the relative error in measuring the diameter of a SWCNT can be about 12% more than that found in the case when the tube axis is perpendicular to electron beam for a 10° tilt and almost 26% smaller than the true diameter. Based on the above result, we recommend to always tilt the tube in the experiment to find the maximum distance between the two dark lines in the HRTEM image or to confine the tube as accurately as possible within the horizontal plane.

We want to make the following notes. In the image of a periodic specimen, although the center of a dark spot may not always correspond to the center of an atom, the period of the image always corresponds to the real period of the crystal. Therefore, the distance between two dark lines or two dark spots in the image correspond to the real plane spacing or atomic distance in the crystal. The present study indicates,

TABLE II. Measurement error resulting from the tilting of the carbon nanotube.

Tilting angle (deg)	0	3.07	5.61	8.38
d measured (nm)	0.475	0.458	0.427	0.412
Relative error (%)	−13.6	−16.7	−22.4	−25.1
Tilting angle (deg)	11.1	16.4	19.5	30.5
d measured (nm)	0.408	0.463	0.432	0.392
Relative error (%)	−25.8	−15.8	−21.5	−28.7

however, that this is not always true for an aperiodic object such as a SWCNT. Among other differences, the atomic plane to the left side of the tube curves toward the right side, while that to the right side of the tube curves oppositely to the left side of the tube. One would expect that the shift between the image and the specimen will be opposite at the two sides of the tube.

C. General phase contrast images

The phase contrast is very sensitive to the experimental imaging conditions such as the defocus condition. Inserted in Fig. 9 are some experimental images of the same part of a SWCNT which were taken at different defocus values. The objective aperture used for obtaining Fig. 9 is around 0.8 Å^{-1}. The contrast in these pictures is mainly phase contrast. The defocus values shown in the figure are relative values. Figure 9 shows indeed the same carbon nanotubes as those shown in Fig. 1. But unlike the inserted images shown in Fig. 1, the contrast of the SWCNT image here results mainly from interferences between the the transmitted and diffracted electron beams and appears to be very different at different defocus values. The part of the tube we used for this set of images is different from that used in obtaining Fig. 1. Our samples of CNT's were from the same source as Ref. 11 which were determined by combined HRTEM and Raman spectroscopy to be of the (n,n) type, with n ranges from 8 to 11.[21] The experimental images of SWCNT's shown in Fig. 9 agrees with a (10,10) tube.

Image simulations are performed for a (10, 10) SWCNT and 200 KeV primary beam energy in order to compare with the experimental images. The results are shown in Fig. 10. The first image map marked as prj is the projected potential. The number on the right hand side of each image is the corresponding underfocus value used in the simulation. This figure shows clearly that the contrast from the SWCNT changes dramatically as the defocus changes, and the typical two dark lines contrast may reverse at small defocus values, e.g. at $\Delta f = -144.5$ Å. This phenomenon also appears in our experiment images as shown in the first inserted image in Fig. 9. The simulated series of images fit well with our experimental images if we add an additional -433.5 Å defo-

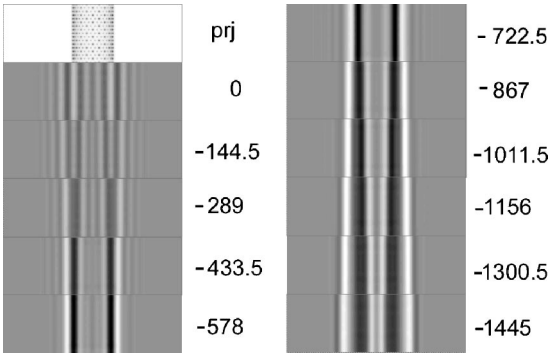

FIG. 10. Simulated high resolution images of a (10, 10) SWCNT. The first image is the projected potential. The number on the right side of each image is the corresponding defocus value in Å.

cus value to that read from the electron microscope panel (very accurate relative defocus values between successively images may be read directly from the electron microscope, although it is difficult to determine the absolute value solely from experiments). The absolute defocus value of the first experimental image shown in Fig. 9 is therefore assigned to $\Delta f = -144.5$ Å.

The distance between the centers of the two dark lines (or white lines when the contrast is reversed) appearing in the images shown in Figs. 9 and 10 is measured as a function of the underfocus values. The results are plotted in Figs. 11 and 12. Figure 11 shows the CNT diameter measured from experimental images as a function of defocus values (corrected based on image simulations). Figure 12 shows the diameter of a (10, 10) SWCNT measured from the simulated images for different values of underfocus. When the corresponding underfocus value is smaller than 60 nm, the diameter measured from experimental images or from simulated images is almost the same as that measured at Scherzer defocus. When the underfocus value is larger than 70 nm, the diameter measured from the experiment image is about 6% smaller than that at Scherzer defocus. In the simulation, the situation is somewhat more complicated. It has been shown in Fig. 10 that for larger underfocus value, the dark lines are broader.

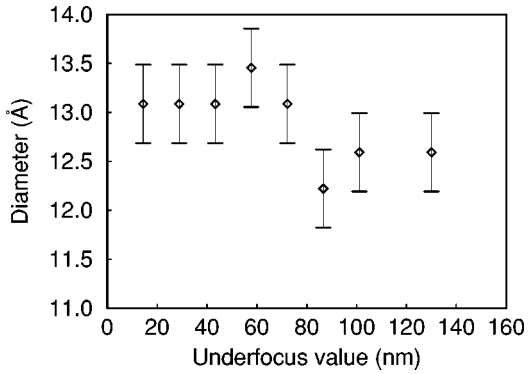

FIG. 11. Measured diameters of a SWCNT using experimental images taken at different defocus conditions. The defocus values have been corrected based on image simulation for a (10, 10) SWCNT.

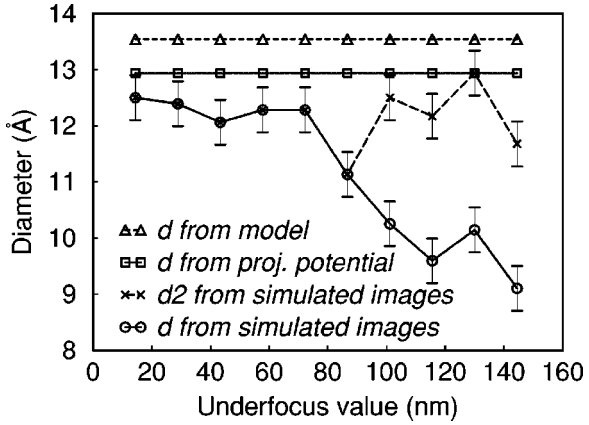

FIG. 12. Diameters of a (10, 10) SWCNT measured from simulated images. The curve marked by d is measured from the centers of the darker part of the dark lines, and that marked by $d2$ is measured from the centers of the dark lines of the SWCNT images.

However, the contrast within the dark line is not uniform being darker near the center of the broad line. The d value in Fig. 12 is measured from the center of the darker part within the broad dark line, while $d2$ is measured from the center of the whole dark line. In real experimental images, however, it is not easy to distinguish contrast variation inside the dark line. On the other hand, the edge between the white and the dark lines is not so sharp on the side far from the tube center. This may make the personally judged center of the broad line move toward the center of the tube, and explains the displayed phenomenon that the measured diameter from experimental images lie between d and $d2$ measured from simulated images. We want to emphasis here that all these measured diameters are smaller than the real diameter of the SWCNT studied. The difference has been discussed in the previous section.

IV. DISCUSSIONS AND CONCLUSIONS

Carbon nanotubes may be imaged either via amplitude or phase contrast mechanisms. When a small objective aperture is used, which excludes all except the transmitted electron beam, the image contrast of a CNT is dominated by the amplitude contrast and the measured value of the carbon nanotube diameter changes hardly as the defocus value varies. When a large objective aperture is used in imaging the CNT, on the other hand, the image of the CNT is formed mainly via interference between transmitted and diffracted electron beams and the image contrast is dominated by the phase contrast. In general, the phase contrast image of a CNT depends sensitively on the defocus value used in imaging, and the main contrast features may reverse in going from underfocus to overfocus.

When a SWCNT is imaged via phase contrast at Scherzer defocus, the image of the tube is dominated by two dark lines which are associated with the two walls of the SWCNT toward the edges of the tube lying nearly parallel to the incident electron beam. An estimation of the diameter of the tube may be made by assuming that the distance between the two dark lines in the image equals the diameter of the tube.

For tubes with diameters larger than say 1.0 nm, this estimation agrees to within 10% of the true value of the carbon nanotube diameter. For tubes with diameter smaller than 1.0 nm, however, the error introduced in this procedure may be as large as 30%. We have shown that an intrinsic error contributes to the inaccuracy in the measurement of the diameter of the CNT, and this intrinsic error cannot be eliminated even a super high-resolution electron microscope is used in imaging the CNT. Briefly, the intrinsic error results from the fact that the best an electron microscope can image is the projected electrostatic potential distribution of the CNT, and for a general tube the minimums in the projected potential do not coincide with the positions of the outmost atoms of the CNT which are usually employed in defining the diameter of the CNT.

When measuring the diameter of a CNT, the tube is usually assumed to lie in a horizontal plane which is perpendicular to the incident electron beam direction. However, the relative orientation of the tube with respect to the incident electron beam is still not well defined in the sense that the tube can rotate about the tube axis and this uncertainty in the rotation angle may introduce finite error in the measurement of the diameter of the tube, e.g., 7% for a (4,4) nanotube. The situation may become even more complicated when the axis of the tube is titled away from the horizontal plane. On the one hand, this tilt introduces variation in the ''height'' of the carbon nanotube and effectively this may be taken into account by introducing an effective defocus value which varies linearly along the tube axis. Typically this extra variation in the ''height'' or effective defocus value is less than a few nanometer and does not introduce substantial additional error in the measurement of the diameter of the CNT's. On the other hand, by tilting the tube axis the crystallographic orientation of the atomic planes of the carbon nanotube may change considerably and introduce additional measurement error which can be as large as 15% . By carefully tilting the carbon nanotube, this additional error may in principle be eliminated. But in practice this is not always so trivial a task. A rule of thumb is to tilt the tube so that a maximum distance between the two dark lines is found, and for Scherzer images this distance represents the most accurate measurement of the tube diameter.

When a high-resolution phase contrast image of a SWCNT is formed, the SWCNT will not always appear as two dark lines and in general the image contrast depends sensitively on the imaging conditions and in particular the defocus value used in imaging. Although the image contrast may reverse from large underfocus to small underfocus and become very complicated for overfocus conditions, the image of a SWCNT appears basically as two dark lines and the two lines become broader as the defocus value deviates from the ideal Scherzer value.

In summary, the diameter of a SWCNT cannot be measured accurately from TEM images. Intrinsic errors exist which make the two dark lines usually observed in experimental TEM images of the SWCNT's narrower than the true tube. These intrinsic errors depend on the relative orientation of the CNT with respect to the incident electron beam but not imaging condition used for obtained TEM images, and may cause errors which is typically less than 10% for tubes with diameters larger than 1.0 nm and as large as 30% for the smallest carbon nanotubes.

ACKNOWLEDGMENTS

The authors thank Professor Z.N. Gu for providing the samples of CNT's and for Professor X. F. Duan for his advices on the use of Philips FEG transmission electron microscope. This work was supported by the National Science Foundation of China, Peking University and the Chinese Academy of Sciences.

*Author whom correspondence should be addressed. E-mail address: lmpeng@blem.ac.cn or plm@ele.pku.edu.cn

[1] Sumio Iijima, Nature (London) **354**, 56 (1991).
[2] Noriaki Hamada, Shin ichi Sawada, and Atsushi Oshiyama, Phys. Rev. Lett. **68**, 1579 (1992).
[3] A. M. Rao and E. Richter, Science **275**, 187 (1997).
[4] Shunji Bandow, S. Asaka, Y. Saito, A. M. Rao, L. Grigorian, E. Richter, and P. C. Eklund, Phys. Rev. Lett. **80**, 3779 (1998).
[5] M. Sugano, A. Kasuya, K. Tohji, Y. Saito, and Y. Nishina, Chem. Phys. Lett. **292**, 575 (1998).
[6] Jeroen W. G. Wildoer, Liesbeth C. Venema, Andrew G. Rinzler, Richard E. Smalley, and Cees Dekker, Nature (London) **391**, 59 (1998).
[7] X. B. Zhang, X. F. Zhang, S. Amelinckx, G. Van Tendeloo, and J. Van Landuyt, Ultramicroscopy **54**, 237–249 (1994).
[8] L. C. Qin, T. Ichihashi, and S. Iijima, Ultramicroscopy **67**, 181 (1997).
[9] D. Bernaerts, M. Op DE Beeck, S. Amelinckx, J. Van Landuyt, and G. Van Tendeloo, Philos. Mag. A **74**, 723 (1996).
[10] X. F. Zhang, X. B. Zhang, G. Van Tendeloo, S. Amelinckx, and M. Op De Beeck, J. Cryst. Growth **130**, 368 (1993).
[11] Z. Shi, Y. Lian, X. Zhou, Z. Gu, Y. Zhang, S. Iijima, L. Zhou, K. Yue, and S. Zhang, Carbon **37**, 1449 (1999).
[12] David B. Williams and C. Barry Carter, *Transmission Electron Microscopy* (Plenum Press, New York, 1996), p. 351.
[13] David B. Williams and C. Barry Carter, *Transmission Electron Microscopy* (Plenum Press, New York, 1996), p. 441.
[14] John M. Cowley, *Diffraction Physics*, 2nd ed. (North-Holland, Amsterdam, 1990).
[15] J.C.H. Spence, *Experimental High Resolution Electron Microscopy* (Oxford University Press, Oxford, 1988).
[16] M. Haider, S. Uhlemanna, E. Schwan, H. Rose, B. Kabius, and K. Urban, Nature (London) **392**, 768 (1998).
[17] L.F. Sun, S.S. Xie, W. Liu, W.Y. Zhou, Z.Q. Liu, D.S. Tang, G. Wang, and L.X. Qian, Nature (London) **403**, 384 (2000).
[18] L.-M. Peng, Z.L. Zhang, Z.Q. Xue, Q.D. Wu, Z.N. Gu, and D.G. Pettifor, Phys. Rev. Lett. **85**, 3249 (2000).
[19] L.C. Qin, X. Zhao, K. Hirahara, Y. Miyamoto, Y. Ando, and S. Iijima, Nature (London) **408**, 50 (2000).
[20] N. Wang, Z.K. Tang, G.D. Li, and J.S. Chen, Nature (London) **408**, 50 (2000).
[21] Z. Shi, Y. Lian, X. Zhou, Z. Gu, Y. Zhang, and S. Iijima, Solid State Commun. **112**, 35 (1999).